Preprint
UCRL-JC-143638

Rock Physics Interpretation of P-wave Q and Velocity Structure, Geology, Fluids and Fractures at the Southeast Portion of the Geysers Geothermal Reservoir

P.A. Berge, L.J. Hutchings, J.L. Wagoner and P.W. Kasameyer

U.S. Department of Energy

Lawrence Livermore National Laboratory

This article was submitted to Geothermal Research Council 2001 Annual Meeting, San Diego, California, August 26-29, 2001

April 6, 2001

Geothermal Res. Council, Transactions, **14**, 2001 Annual Meeting, San Diego, CA.

Rock Physics Interpretation of P-wave Q and Velocity Structure, Geology, Fluids and Fractures at the Southeast Portion of The Geysers Geothermal Reservoir

Patricia Berge, Lawrence Hutchings,

Jeffrey Wagoner, and Paul Kasameyer

Energy and Environmental Directorate

Lawrence Livermore National Laboratory

P.O. Box 808

Livermore, California 94551

April 6, 2001

Abstract

We examine how quantitative rock physics models, such as effective medium theories, can improve the interpretation of seismic parameters and material and fluid properties at The Geysers. We use effective medium theories to estimate effects of fractures on velocities for The Geysers rocks. We compare theoretical velocity estimates to laboratory measurements from the literature and our seismic velocity values from 1992 earthquake data. We approximate the reservoir as being homogeneous in mineral composition, with a constant density of fractures whose total void ratio is reduced by lithostatic pressure. Thus, we expect low velocities near the surface, increasing with depth up to the values observed in the lab on intact samples, 5.5 - 5.7 km/sec. We use a one-dimensional inversion of P-waves to obtain an “expected” P-wave velocity (*Vp*) and attenuation (*Qp*) relation as a function of depth for The Geysers rocks. We then use a three-dimensional *Vp* and *Qp* inversion to find anomalous zones within the reservoir. We find portions with “high” *Vp* and *Qp*, high *Vp* and low *Qp*, and low *Vp* and low *Qp*. We interpret the regions with high *Vp* and *Qp* to be relatively less fractured, and the regions with low *Vp* and *Qp* to be significantly fractured. The high V and Q anomaly is centered on the zone of greatest pressure drop, and is mostly within the shallowest part of the felsite. The anomalous zones within the graywacke reservoir are on either side of the felsite, in areas of more moderate pressure depletion. More work is required to interpret the significance of these observations.

Introduction

One of the clearist observables in a geothermal field is the microseismicity associated with the production, injection and flow of fluids in the subsurface. Although previous studies have made general interpretations of the relation of reservoir properties to observable seismic parameters, few studies have made an attempt to obtain a fundamental understanding of the relationship between seismic parameters and material and fluid properties at The Geysers. This requires moving away from empirical approaches and taking a comprehensive perspective. We are currently examining how quantitative rock physics models, such as effective medium theories, can improve the interpretation of these data. In this paper we use rock physics theories that relate rock composition, porosity, fractures, and fluids to seismic velocities to identify the state of fluids and fractures in the geothermal reservoir.

We utilize recordings of microearthquakes for the period January 1992 through August 1992, prior to the beginning of the Unit 18 Cooperative Injection Test in December 1993, in this interpretation. We have determined the locations and source characteristics for 200 earthquakes with magnitude about 0.8, performed tomographic inversions for 3-D models of P-wave velocity (*Vp*) and P-wave attenuation (*Qp*). In this paper, we 1) use laboratory data and these observations to show that the primary factor influencing *Vp* variations is the extent of open fractures, 2) determine the average velocity- and attenuation-depth profiles that are consistent with this model, and 3) identify areas where both *Vp* and *Qp* are anomalous compared to this profile. In future work, we intend to add observations of stress drop from the microearthquakes to this data set, evaluate the possible effects of saturation variations on *Vp* and *Qp*, and determine if we can estimate fracture spacing within the field.

We utilize three-dimensional plotting capabilities from earthVision (earthVision5.1™ software) to understand spatial associations and cross-correlations of reservoir properties. Figure 1 shows the study area. Also shown on Figure 1 are reservoir pressure contours obtained from individual observation wells and field-wide isobaric maps for April 1991 (Pham and Menzies, 1993), during the period of this study.

Geology

In the southeast Geysers Geothermal Field the steam-producing reservoir host rock is a Jurassic-Cretaceous Franciscan graywacke and a younger Pleistocene felsite intrusive rock. Overlying the reservoir is a cap rock, a melange of metamorphic Franciscan rocks that are cut by Mesozoic and earlier, low-angle thrust faults (Thompson, 1991). The cap rock is up to about 1,200 m (4000 ft) thick. Thompson suggests a roughly antiformal structure of the felsite dominating the overall shape of the reservoir and possible stream migration to the apex of the antiform. Figures 4 shows the three-dimensional shape of the graywacke; the melange and felsite are above and below the graywacke, respectively.

Previous Work

Fluids', fractures' and pores' effect on velocities are important at all scales. However, the pores are only significant at ultrasonic wavelengths, whereas the fractures that affect seismic velocities at the field scale are not present in a core sample used for laboratory ultrasonic measurements. Further, an important consideration is that although Gassmann's theory (1951) predicts no change in shear modulus in a porous medium due to change in fluid properties, effective medium theories do predict such changes because they include effects of void geometry that control resolution of the stress field at the scale of the void space, i.e. Poisson effect (Berryman, 1999; Berryman and Wang, 2000; Berryman et al., 2001).

Boitnott (1995) and Boitnott and Boyd (1996) made laboratory measurements of ultrasonic compressional and shear wave velocities for dry and fully saturated core samples from The Geysers reservoir and cap-rock metagraywacke and argillite at confining pressures from 0 to 90 MPa. The cores were recovered from depths of -2599 m (-8,526 ft) to -2602 m (-8536 ft) in the NEGU-17 drill hole. The samples included 6 metagraywacke plugs with porosities of 1 to 2 percent, a metashale sample with porosity of about 2 percent, and a highly altered metagraywacke plug with porosity of about 8 percent in the form of macropores. They found that saturation of pores resulted in an increase in *Vp/Vs* ratios, due primarily to an increase in *Vp*. Boitnott (1995) qualitatively interpreted the change in *Vp* as a result of a chemo-mechanical weakening of the shear modulus with saturation. White (1975) also reported an increase in seismic *Vp* with saturation, while *Vs* remained unchanged. Romero (1995) interpreted White's results as being due to liquid causing the stiffness specific to compressional waves to increase, while not inhibiting the relative shear displacement across joints. Boitnott and Boyd also found that velocities did not increase significantly with pressure, indicating that the core samples do not contain significant amounts of microcracks.

Several researchers have constructed seismic velocity and attenuation images of the Geysers geothermal field, located seismicity, and interpreted the significance of seismicity and its relation to steam production. No previous studies have produced high resolution Q images of the southeast Geysers. Kirkpatrick et al. (1999) studied microearthquake occurrence in the same area as this study, with the same station locations, for the period January 1994 through 1998, during the time of the Unit 18 Cooperative Injection Test. Kirkpatrick et al. found that in the area of the injection test seismicity rates, injection rates, and production rates correlated very well. Seismicity rates did not initiate until 3 months after injection started, but correlated in time after that. Smith et al. (2000) show that monthly seismicity rates correlate more with injection than with production.

Several studies have performed a three-dimensional block inversion for P-wave and S-wave velocity structure for The Geysers (Majer and McEvilly, 1979; Gupta, *et al*., 1982; Eberhart-Phillips and Oppenheimer, 1984; Eberhart-Phillips, 1986; and O'Connell and Johnson, 1991. The resolution varied from 3 km3 to 1 km3 volume cubes. In this study, we increase resolution to cubes with 0.22 km3 (2000 ft dimension for each side). Kirkpatrick et al. (1997) conducted three-dimensional *Vp* and *Vs* inversions for the same portion of The Geysers area as studied here. Interpretation is complicated by the transition with depth from metagraywacke-dominated to felsite-dominated matrix. However, they found that high *Vp* values correlated with high *Vs* and low *Vp* correlated with low *Vs* in the metagraywacke. Effective medium theories would suggest that low *Vp* and *Vs* indicate highly fractured regions, while high *Vp* and *Vs* may indicate unfractured regions. At greater depths, thought to coincide with the felsite, Kirkpatrick et al. found positive correlation between high *Vp/Vs* and high *Vp*. They did not do fluid substitution modeling (e.g., Gassmann, 1951) or effective medium theory modeling (e.g., Berryman, 1995) to constrain fluid effects on rock velocities.

Predictions from Effective Medium Theory

The seismic parameter estimates provide information that can be used for quantitative estimates of effects of stress changes, fluids, and fractures on seismic velocities and attenuation. The approach used is to perform numerical modeling using effective medium theories (e.g., Berryman, 1995) and other theoretical methods, to quantify how velocities and attenuation change for given changes in fracture concentration, porosity, fracture or pore fluid content, mineralogy, and scale of measurements (i.e. lab vs. field).

We compare the theoretical predictions with observed velocities and available lab data. Further work will include modeling attenuation.

Previous studies such as Zucca et al. (1994) have interpreted velocity and attenuation images based upon laboratory data on the response of typical oil-field rocks such as Berea sandstone. However, laboratory measurements on cores from The Geysers show that they do not respond in the same way. Figure 2a shows laboratory P- and S-wave velocity results from Boitnott (1995) plotted against void ratio. Figure 2a shows that 1) for the Westerly granite (first data points on far left), the *Vp* increased while *Vs* increased slightly with saturation; 2) for The Geysers (NEGU-17) *Vp* increased while *Vs* did not change or decreased slightly with saturation; 3) highly altered Geysers graywacke showed *Vp* increased slightly while *Vs* did not change; and 4) Berea ss has a significantly different void ratio, and *Vp* increased and *Vs* decreased slightly with saturation. Thus, there is really no known analog for The Geysers metagraywacke.

We can improve our understanding of the fluid effects on velocities by replotting the Boitnott lab measurements in terms of bulk and shear modulus rather than *Vp* and *Vs*, to remove the well-known effects of fluids on density (Figure 2b). Figure 2b shows that 1) for the Westerly granite, the bulk modulus increased significantly while the shear modulus increased slightly with saturation; 2) for The Geysers (NEGU-17) the bulk modulus increased significantly while shear modulus decreased slightly with saturation; 3) highly altered Geysers graywacke showed the bulk modulus increased significantly while the shear modulus increased slightly with saturation, and 4) for Berea ss the shear modulus did not change and the bulk modulus increased. This emphasizes that the behavior of the Berea sandstone is not like the behavior of the Geysers samples, and the behavior of the Westerly granite is not like any of the Geysers samples except for the highly altered metagraywacke sample. We note that the large differences in dry and saturated bulk modulus values for the lowest porosity Geysers samples are probably due to chemical effects of fluids in the rock.

Field seismic studies have found much lower velocities than those measured in the laboratory (e.g. Zucca et al., 1994). The discrepancy is due to fractures. We can use effective medium theories to estimate effects of fractures on velocities for The Geysers rocks. An appropriate effective medium theory for estimating velocities in low-porosity igneous rocks containing fractures is the differential effective medium (DEM) theory (e.g., Berge et al., 1991). At low fracture concentrations, other theories such as the Kuster-Toksoz (1974) model and the self-consistent (SC) effective medium theory of Berryman (1980) yield results that are close to the DEM results. We can also find the Hashin-Shtrikman (HS) bounds on velocities and moduli (Hashin and Shtrikman, 1963). The Geysers rocks are a mixture of minerals, pores, and fractures, with quartz and feldspar as the dominant minerals. Since we do not have a zero porosity laboratory sample, we use bulk and shear moduli of the minerals for an assumed mixture of the minerals to represent properties of the zero-porosity, unfractured case. Quartz has a bulk modulus of about 38 GPa and a shear modulus of about 44 GPa, whereas feldspar has a bulk modulus of about 70 GPa and a shear modulus of about 30 GPa. By plotting the HS bounds for various mixtures of quartz, feldspar, and adding pores for porosities between 0 and 10 percent and comparing to lab measurements of the metagraywackes from The Geysers, we find that a mixture of about 50 percent quartz and 50 percent feldspar will yield correct values for the low porosity samples from The Geysers. This is our starting model for unfractured rock, a material with bulk modulus of about 55 GPa and shear modulus of about 35 GPa. Changing the proportions of quartz and feldspar by a few percent will not change the modeling results significantly. We alternatively could have used the highest measured laboratory values for the moduli (53 and 33 GPa), which would mean ignoring the effects of the small amount of porosity present in the cores. Note that the zero porosity value would be the same for the dry or saturated case unless there are chemical effect of the fluid on the rock.

Figures 3 shows predicted dry bulk modulus from the DEM theory. The pores have aspect ratio of 1.0, cracks intermediate aspect ratio below 1.0 (0.1), thin cracks (fractures) have very low aspect ratio (.01 - .001). The flatter the cracks, the more the moduli and velocities decrease, even for small amounts of cracks. It is clear from the figure that the very low aspect ratio cracks can produce very significant changes in the bulk moduli and velocity, even for rocks with very low void ratios. Clearly, the seismic velocities can be explained by fractures lowering velocities compared to measured laboratory values. Also note that fractures and cracks will close with depth, leading to an increase in seismic velocity with depth. Thin cracks or fractures close at shallower depths, and eventually all cracks or fractures close.

These observations lead to an “expected” distribution of the velocity with depth at The Geysers. At this time we will consider only the effects of pressure closing the low aspect ratio cracks on Vp. (Modeling effects of saturation and chemical changes will be evaluated in the future). The mineralogical changes are not dramatic through the reservoir; for example, there are no carbonates or basaltic rocks. To determine an "expected" velocity-depth profile, we will approximate the reservoir as being homogeneous in mineral composition, with a constant density of fractures whose total void ratio is reduced by lithostatic pressure. Thus, we expect low velocities near the surface, increasing with depth up to the values observed in the lab on intact samples, 5.5 - 5.7 km/sec. Once this value is reached, then there would be no more velocity increase with depth. Rather than speculating on the fracture spacing and initial void ratio, we will determine this depth and the initial velocity for the "expected" velocity/depth curve from a 1-D inversion of our field data. Since we have not modeled Qp yet, a similar assumption will be used for the *Qp*/depth curve. By identifying parts of the reservoir volume that do not match this expected curve, we can find regions that are anomalous either in fracture density and spacing, fluid saturation or mineralogy.

Methods

Once we have established a model for the "expected" seismic velocity and attenuation as a function of depth for The Geysers, we will utilize seismic inversion to identify variations of velocity and attenuation as compared to the model to identify anomalous zones. We used the Thurber (1983) inversion code, modified by Eberhart-Phillips (1986) and further modified to include inversion for *Qp* (Zucca et al., 1994). We invert travel times to obtain three-dimensional models of P-wave velocity. We perform inversion of pulse widths, obtained from initial P-waves of the time series, to obtain three-dimensional models of *Qp* structure. Several researchers have used spectral ratios to invert for Q structure in geothermal and volcanic areas (e.g., Ho-Liu et al., 1988; Sanders 1984; Ward and Young 1985; Evans and Zucca, 1988; and Romero, 1995). Zucca et al. (1994) and Lees et al. (1995) used pulse-widths to invert for Q structure. The inversion of pulse widths is absolute and can be traced by the same rays used for P-velocity inversion to points within the column.

Data

Data used for this study are digitized seismograms obtained from three simultaneously operated networks, the LLNL, LBL, and Unocal networks. The Unocal network (now operated by Calpine Corp) has operated in The Geysers area since 1985. The purpose of the LLNL and LBL networks was to provide high resolution digital recordings of microearthquakes from closely spaced stations. LLNL and LBL operated companion microearthquake recording networks in the southeast Geysers geothermal area from July 1991 to September 1993. Several of the LBL stations were co-located with Unocal stations.

Data processing consisted of combining three data sets. Unocal provided first arrival picks for Unocal-operated network stations (M. Stark, personal communication, 1992). All available Unocal first P-wave arrival times were used for the velocity structure and earthquake location inversion. Unocal arrival pick accuracy was greater than or equal to +/- 0.01 seconds since the records were digitized at 100 samples per second. The Unocal data was used for velocity inversions and the LBL data was used to obtain P-wave pulse widths for the *Qp* inversions. The LLNL data was used for both velocity and pulse width inversions.

The grid system used in this study is organized so that nodes fall at the middle of the Unocal-NEC-Thermal (UNT) grid system UNT grid cubes. The grid nodes for this study are shown in Figure 1. In the following discussions depths are reported at negative values from mean sea-level. The first node point of the present study area (southern point) is at x = 305 m (1000 ft) and y = 915 m (3000 ft) of the UNT system. Since the horizontal and vertical grid spacing is 610 m (2000 ft), this puts a node in the middle of each 610 m (2000 ft) cube of the UNT block grid system. We use a node grid of 3.05 km (10,000 ft) along the x-axis and 3.67 km (12,000 feet) along the y-axis, and vertically, from z = 915 m (3000 ft) above sea-level, to -1,830 m (-6,000 ft) below sea level. The study area shown in Figure 1 is oriented askew to the grid system, but contains the portion of the study area that has significant resolution for interpretations. The nodes for this study are shown in Figure 1.

Inversion Results

The starting velocity model for the velocity inversion used here was obtained by modifying the results from the previous study Zucca et al. (1994) in the portion of The Geysers to the immediate northwest. The average of the three dimensional model from Zucca et al. (1994) was used to invert for a one-dimensional model based upon the southeast Geysers data. This final one-dimensional model was used as the starting model for the three dimensional inversion of this study. The velocity inversion achieved a 40% reduction in variance of the observed and predicted travel times when compared with those obtained from the starting model. All but 6% of this reduction is due to relocating the earthquakes. Diagonal resolution values range up to about 0.1. Plots of the values of the row elements of the resolution matrix indicate that diagonal elements with values greater than 0.05 have at least a 20:1 ratio to off-diagonal elements, and this is taken as a better indication of the resolution. With this criterion, most of the nodes in teh central portion of hte studya area (outlined by teh pressure contours in Figure 1) are well resolved for depths of 305 m (1000 ft) to -1,525 m (-5000 ft). The average standard error of node values is 0.07.

The final one-dimensional model discussed above was also used to determine our "expected" velocity-depth curve caused by closing of fractures. We fit it with two straight-line segments: a constant value, 5.5 km/s, consistent with the lab measurements, below elevations of -2000 m, and a constant slope starting at 4.0 km/sec at the surface meeting that line at 2000m. These are much larger velocity changes with pressure than were produced by saturation changes in the lab, and probably reflect that closing fractures dominates the velocity structure at this part of The Geysers. Figure 4 shows the ratio of the velocity inversion results to that "expected" model at depths corresponding to the surface of the greywacke.

The starting *Qp* model was obtained by first using an average *Qp* for the structure obtained by a straight line fit to pulse widths; this gave a *Qp* of 65. This was used to obtain a one dimension *Qp* model, which was the starting model for the three-dimensional *Qp* velocity. The inversions for Qp had a better ratio of observations to free parameters than the travel time inversions had since the locations of the earthquakes were held fixed. However the data were much more noisy, so that the quality of the inversions was not as good as for velocity structure. The first iteration included source duration calculations resulted in a 33% decrease in variance. After the source duration stabilized there was an additional 5% decrease in variance. The *Qp* resolution values were greater than those for the Vp inversion, primarily because of fewer free parameters in the inversion. Still, diagonal resolution values of 0.05 or greater generally had a ratio of 10:1 to off-diagonal elements. In the following discussion, only nodes with a *Qp* diagonal resolution of 0.05 or greater were considered.

We fit the one-dimensional *Qp* model with two straight lines intersecting at -2000m elevation to determine our "expected" *Qp* model, which starts at 20 at the surface and increases to about 40 at an elevation of -2000 m. Figure 5 shows the ratio of the *Qp* in the inversion divided by the "expected" *Qp* and plotted on the surface of the Graywacke.

We have chosen the following criteria to define "anomalous" areas: *Vp* differs from the expected value by more than 5% and *Qp* differs from the expected value by more than 50%. These criteria are somewhat arbitrary. We also required the resolution matrix to meet the criteria discussed above. At this time, we have not attempted to determine whether the anomalous values are caused by anomalous fracture density and spacing, saturation differences or mineralogy differences. Figure 6 shows the portions of the study area where we detected both high *Vp* and *Qp* consistent with a reduced fracture density. The anomalies occur at two elevations, about -1000 m, in the melange, and -2000 m, mostly in the felsite. Figure 7 shows areas with high velocity but low *Q*. These occur about -1500m within the graywacke. This may be a combination of fluid and compositional effects. Additional modeling will be required to identify what might cause this type of anomaly. Figure 8 shows areas with low *Vp* and low *Qp*, consistent with a high fracture density. These also occur within the graywacke. No zones were found with low *Vp* but high *Qp*.

Figure 9 provides a map view showing the anomalous zones within the reservoir, and their relationship to the pressure drawdown observed in the year prior to our data collection. The high *Vp* and *Qp* anomaly is centered on the zone of greatest pressure drop, and is mostly within the shallowest part of the felsite. The anomalous zones within the graywacke reservoir are on either side of the felsite, in areas of more moderate pressure depletion. Evaluation of the relationship of these anomalous zones to structural elements, injection or production, and other factors may show that they are diagnostic of important features within the field.

Conclusions

Laboratory measurements and effective medium theories provide a useful framework for the interpretation of tomographic images in geothermal fields. They clearly indicate that inferences based on observations of non-geothermal rocks may not apply to the highly altered materials found in geothermal fields. Anomalous zones can be found that correlate with the area of pressure drawdown in the southeast Geysers, but more work is required to interpret their significance.

Acknowledgments

This work was performed under the auspices of the U.S. Department of Energy by the University of California Lawrence Livermore National Laboratory under contract W-7405-ENG-48 and was supported specifically by the DOE Office of Geothermal and Wind Power Technologies. Data and processing were provided by Unocal Geothermal and by Lawrence Berkeley Laboratory National Laboratory.

References

Berge, P.A., Gerard J. Fryer, and Roy H. Wilkens (1992) Velocity-Porosity Relationships in the Upper Oceanic Crust: Theoretical Considerations. Journal Geophys. Res. **97**, B11, pp 15,239-15,254.

Berryman, J. G. (1995) Mixture theories for rock properties, in *Rock Physics & Phase Relations*, a handbook of Physical Constants, AGU Reference Shelf 3, Thomas J. Ahrens, Editor, American Geophysical Union, Washington, DC, pp 205-228.

Boitnott, G. N. (1995) Laboratory Measurements on Reservoir Rocks from The Geysers Geothermal Field. proceedings, *Twentieth Workshop on Geothermal Reservoir Engineering*, Stanford University, Stanford, California, January 24-26, 1996. SGP-TR-150.

Boitnott, G. N. and P.J. Boyd (1996) Preliminary, Electrical Impedance, and Acoustic Velocities on Reservoir Rocks from The Geysers Geothermal Field. proceedings, *Twenty-first Workshop on Geothermal Reservoir Engineering*, Stanford University, Stanford, California, January 22-24, 1996. SGP-TR-151.

Boitnott, G. N. and Ann Kirkpatrick (1997) Interpretation of Field Seismic Tomography at The Geysers Geothermal Field, California. *Twenty-second Workshop on Geothermal Reservoir Engineering*, Stanford University, Stanford, California, January 27-29, 1997. SGP-TR-155.

Evans, John R. and Zucca, John J. (1988) Active High-Resolution Tomography of compressional-wave velocity and attenuation structure at Medicine Lake Volcano Northern California Cascade Range. submitted to J. Geophys. Res.

Eberhart-Phillips, Donna (1986) Three-dimensional velocity structure in northern California Coast Ranges from inversion of local earthquake arrival times. Bull. Seis. Soc. Am., **76**, 1025–1052.

Eberhart-Phillips, D. and D. H. Oppenheimer (1984) Induced seismicity in The Geysers geothermal area, California, J. Geophys. Res., **89**, 1191–1207.

Foulger, G. R., C.C. Gramt, A Ross, and B.R. Julian (1997) Industrial Induced Changes in Earth Structure at The Geysers Geothermal Area, California. Geoph *Res Let* Vol 24, 135-137.

Ho-Liu, P., H. Kanamori, and R.W. Clayton (1988) Applications of attenuation tomography to Imperial valley and loso-Indian well region, southern California. J. Geophys. Res. 93, 3321–3338.

Julian, B.R., A. Ross, G.R. Foulger, and J.R. Evans (1996) Three-dimensional seismic image of a geothermal reservoir: The Geysers, California. Geoph *Res Let* Vol 23, 685-688.

Kirkpatrick, Ann, John E. Petterson Jr., and Ernest L. Majer (1997) Three-dimensional Compressional- and Shear Wave Seismi9c Velocity Models for the Southeast Geysers Geothermal Field, California. proceedings, *Twenty-second Workshop on Geothermal Reservoir Engineering*, Stanford University, Stanford, California, January 27-29, 1999. SGP-TR-155.

Kirkpatrick, Ann, John E. Petterson Jr., Ernest L. Majer, and Robert Nadeau (1999) Characteristics of Microseismicity in the DV11 Injection Area, Southeast Geysers, California. proceedings, *Twenty-fourth Workshop on Geothermal Reservoir Engineering*, Stanford University, Stanford, California, January 25-27, 1999. SGP-TR-162.

Majer, E. L. and T. V. McEvilly (1979) Seismological investigations of The Geysers geothermal field. Geophysics **44**, 246–269.

O'Connell, Daniel, and Lane R. Johnson (1991), Progressive inversion for hypocenters and P wave and S wave velocity structure: application to The Geysers, California, Geothermal Field, J. Geophys. Res., 96, 6223–6236.

Romero, Jr., Arturo, Espejo (1995) *Application of Seismic Tomographic Techniques in teh Investigation of Geothermal Systems*, PhD. Thesis, University of California, Berkeley.

Smith, J.L., Joseph J. Beall and Mitchel A. Stark (2000) Induced Seismicity in the SE Geysers Field. Geothermal Resources Council, Transactions, Vol. 24, September 24-27, pp. 331-336.

Thompson, R. C., and R. P. Gunderson (1989) The orientation of steam-bearing fractures at The Geysers Geothermal Field, Geothermal Res. Council, *Transactions*, **13**, 487–490.

Thompson, Randolph C. (1991) Structural Stratigraphy and Intrusive Rocks at The Geysers Geothermal Field. in *Monograph on The Geysers Geothermal Field. C. Stone, Ed. Geotherm. Res. Council Special Rept.* 17, 59-63.

Thurber, C. H. (1983) Earthquake locations and three-dimensional crustal structure in the Coyote Lake area, central California, *J. Geophys. Res.*, **88**, 8226–8236.

White, J. E. (1975) Computed seismic speeds and attenuation in rocks with partial gas saturation. Geophysics, vol.40, no.2, pp.224-232, Apr 1975

Zucca, J.J., L.J. Hutchings, and P.W. Kasameyer (1994) Seismic Velocity and Attenuation Structure of The Geysers Geothermal Field, California. *Geothermics* **23**, 111-126.

Figures

Figure 1: Outline of three-dimensional plot area, contours of pressure as of April 1992 (Pham and Menzies, 1993), nodes used to derive *Vp* and *Qp* (crosses), epicenters of earthquake used in this study (dots), and outline of steam field (thin contour).

Figure 2a: Laboratory P- and S-wave velocity measurements at 30 MPa plotted as a function of void ratio (porosity), from Boitnott (1995).

Figure 2b: Bulk and shear modulus plotted as a function of void ratio, using data from Boitnott (1995).

Figure 3: Bulk moduli estimated using the differential effective medium (DEM) theory for various crack shapes and amounts of cracks and pores, for dry case.

Figure 4: Variation of velocity inversion results from the "expected" model as viewed on the graywacke.

Figure 5: Variation of *Qp* inversion results from the "expected" model as viewed on the graywacke.

Figure 6: Portions of volume where *Qp* is greater than 50% above the average model and the *Vp* values are greater than 5% of the average model (red dots), the pressure contours from Figure 1 (blue contours), and the felsite formation (blue shading).

Figure 7: Portions of volume where *Qp* is greater than 50% above the average model and the *Vp* values are less than 5% of the average model (red dots), the pressure contours from Figure 1 (blue contours), and the felsite formation (blue shading).

Figure 8: Portions of volume where *Qp* is less than 50% above the average model and the *Vp* values are less than 5% of the average model (red dots), the pressure contours from Figure 1 (blue contours), and the felsite formation (blue shading).

Figure 9: A map view of the anomalous portions of the reservoir:

Red solid squares are areas in the felsite where *Vp* > 105% and *Qp* > 150% of average.
Green open squares are areas in the graywacke where *Vp* > 105% and *Qp* > 150% of average.
Blue open squares are areas in the graywacke where *Vp* > 105% and *Qp* < 50% of average.
Brown open squares are areas in the graywacke where *Vp* < 95% and *Qp* < 50% of average.

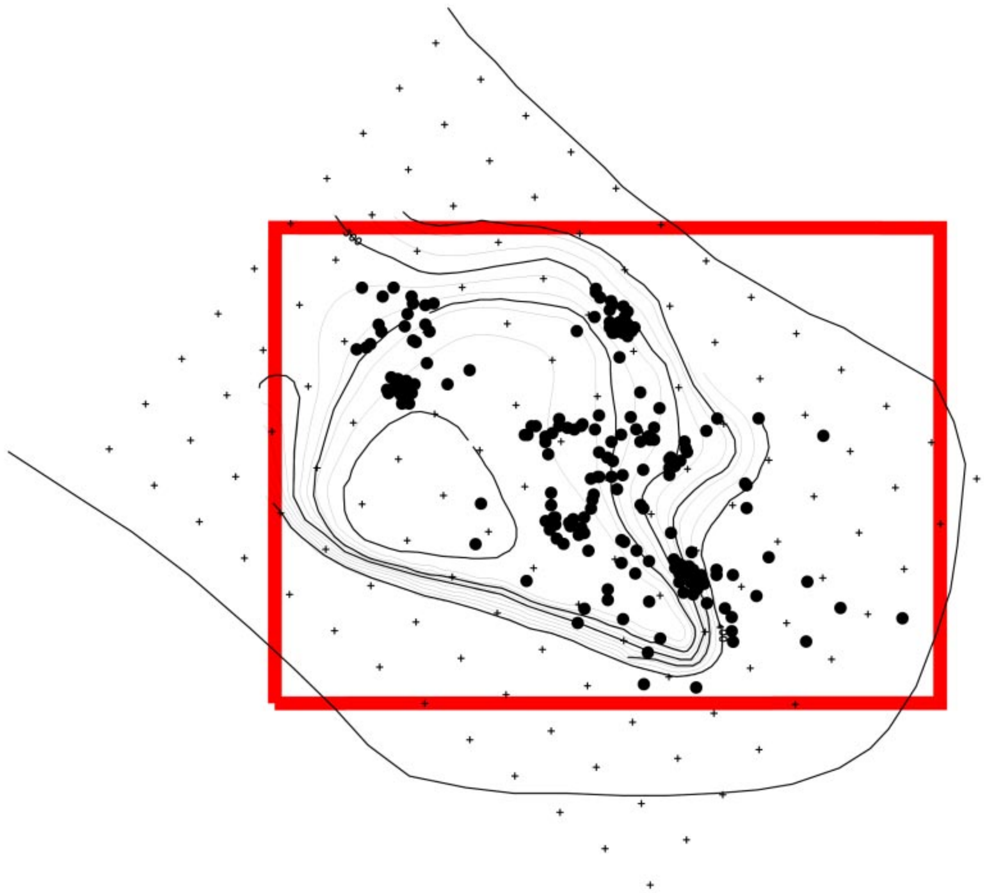

Figure 1

(a)

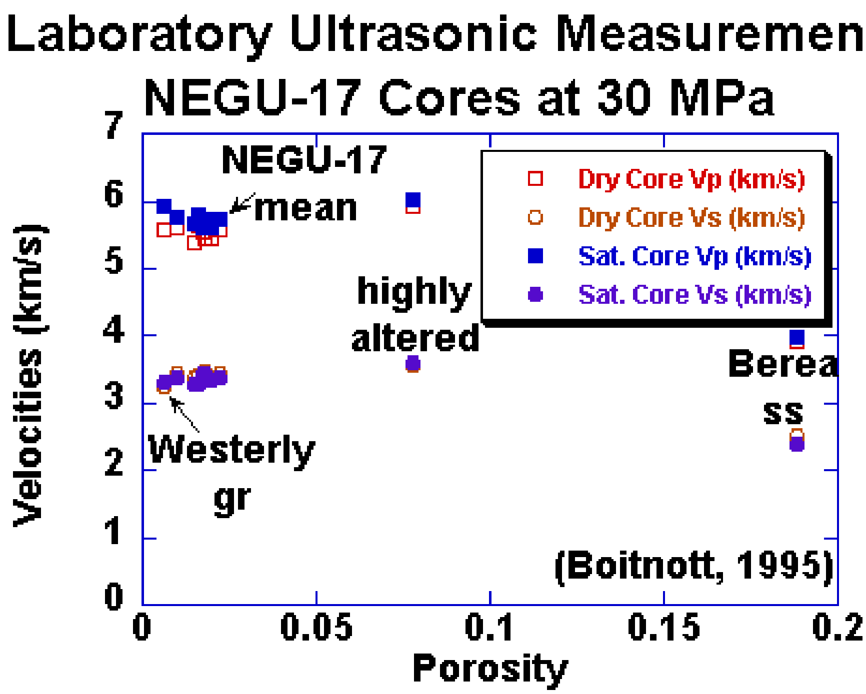
Laboratory Ultrasonic Measurements
NEGU-17 Cores at 30 MPa
Velocities (km/s)
Porosity
0
1
2
3
4
5
6
7
0
0.05
0.1
0.15
0.2
NEGU-17
mean
highly
altered
Westerly
gr
Berea
ss
Dry Core Vp (km/s)
Dry Core Vs (km/s)
Sat. Core Vp (km/s)
Sat. Core Vs (km/s)
(Boitnott, 1995)

(b)

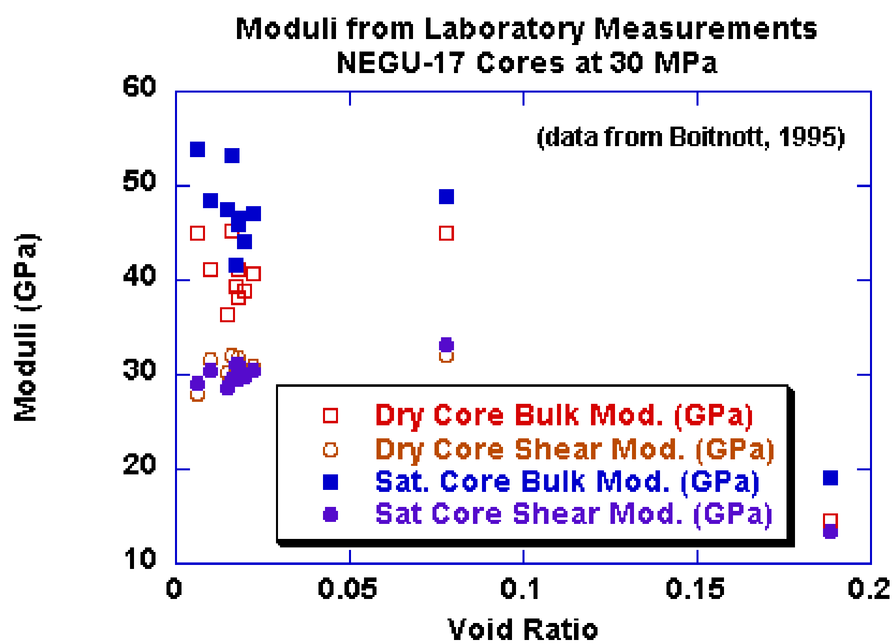
Moduli from Laboratory Measurements
NEGU-17 Cores at 30 MPa
Moduli (GPa)
Void Ratio
10
20
30
40
50
60
0
0.05
0.1
0.15
0.2
(data from Boitnott, 1995)
Dry Core Bulk Mod. (GPa)
Dry Core Shear Mod. (GPa)
Sat. Core Bulk Mod. (GPa)
Sat Core Shear Mod. (GPa)

Figure 2

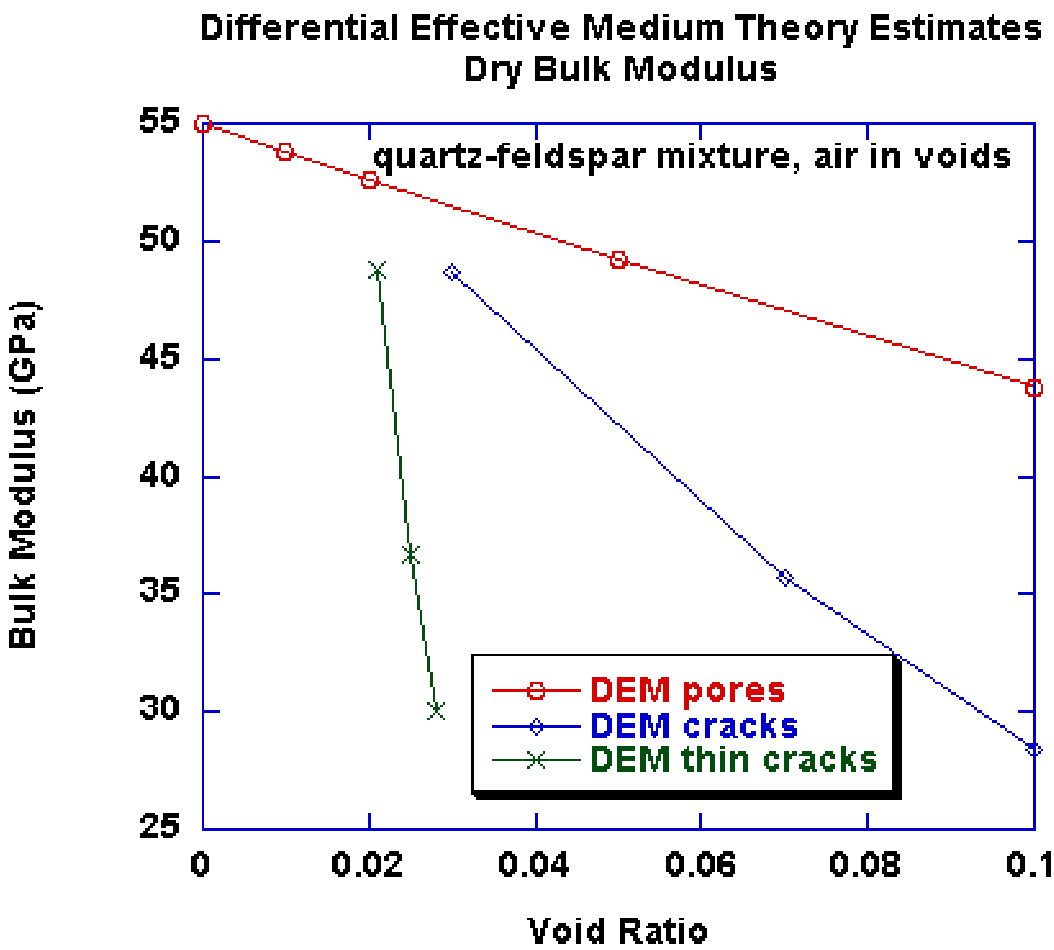
Differential Effective Medium Theory Estimates
Dry Bulk Modulus
quartz-feldspar mixture, air in voids
Bulk Modulus (GPa)
Void Ratio
55
50
45
40
35
30
25
0
0.02
0.04
0.06
0.08
0.1
DEM pores
DEM cracks
DEM thin cracks

Figure 3

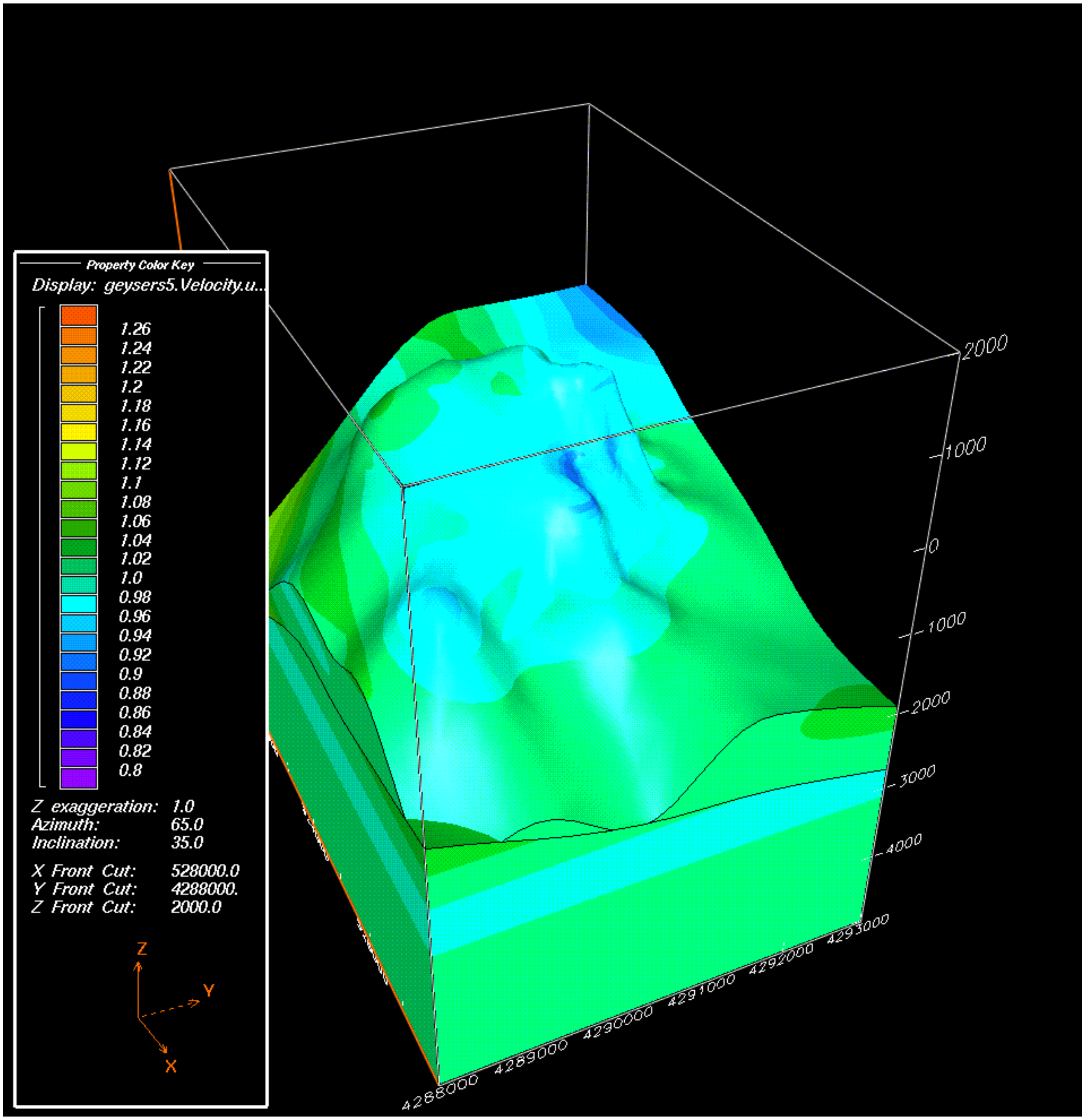

Property Color Key
Display: geysers5.Velocity.u...
1.26
1.24
1.22
1.2
1.18
1.16
1.14
1.12
1.1
1.08
1.06
1.04
1.02
1.0
0.98
0.96
0.94
0.92
0.9
0.88
0.86
0.84
0.82
0.8
Z exaggeration: 1.0
Azimuth: 65.0
Inclination: 35.0
X Front Cut: 528000.0
Y Front Cut: 4288000.
Z Front Cut: 2000.0
Z
Y
X
2000
1000
0
-1000
-2000
-3000
-4000
4288000
4289000
4290000
4291000
4292000
4293000

Figure 4

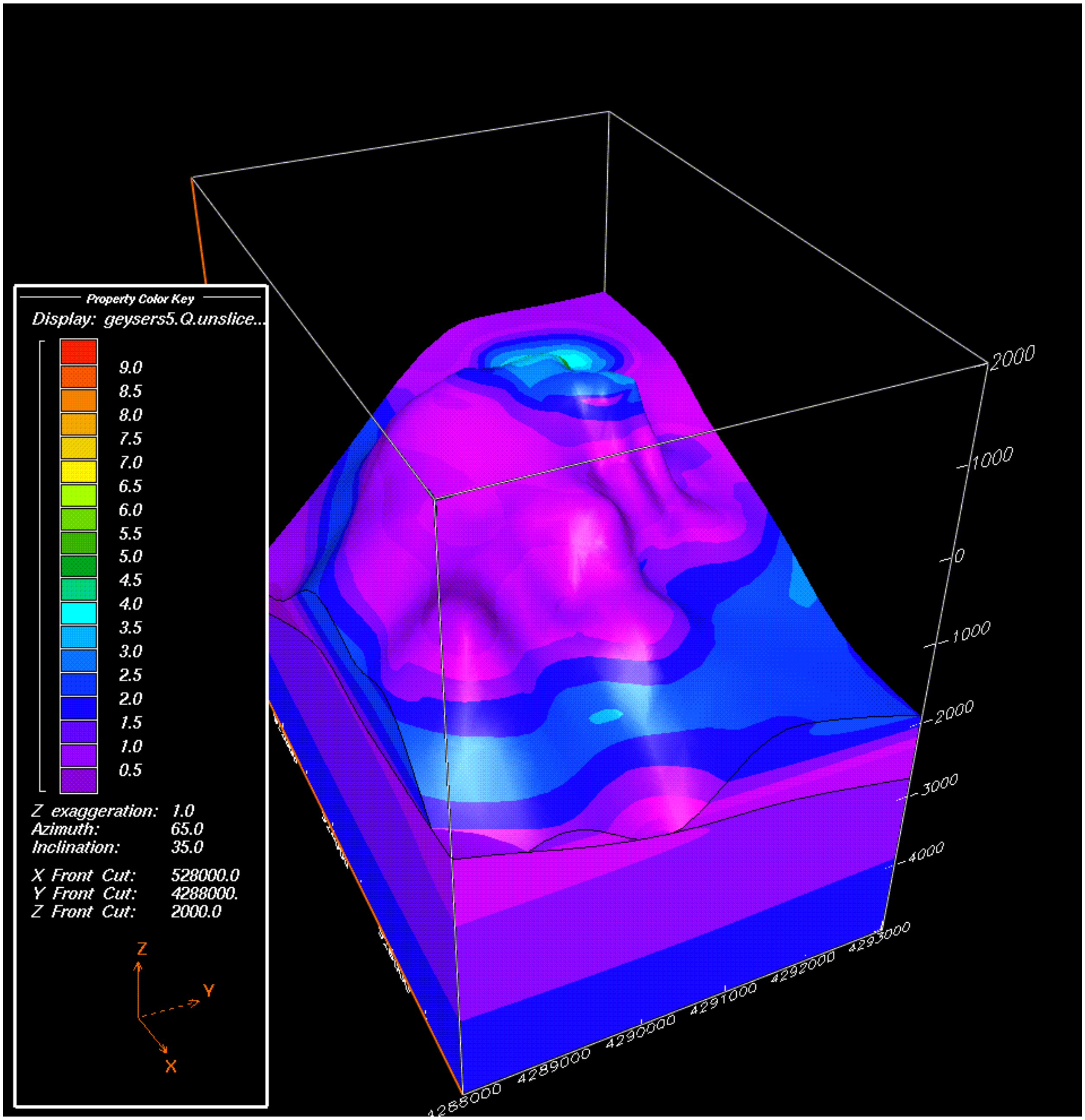
Property Color Key
Display: geysers5.Q.unslice...
9.0
8.5
8.0
7.5
7.0
6.5
6.0
5.5
5.0
4.5
4.0
3.5
3.0
2.5
2.0
1.5
1.0
0.5
Z exaggeration: 1.0
Azimuth: 65.0
Inclination: 35.0
X Front Cut: 528000.0
Y Front Cut: 4288000.
Z Front Cut: 2000.0
Z
Y
X
2000
1000
0
-1000
-2000
-3000
-4000
4288000
4289000
4290000
4291000
4292000
4293000

Figure 5

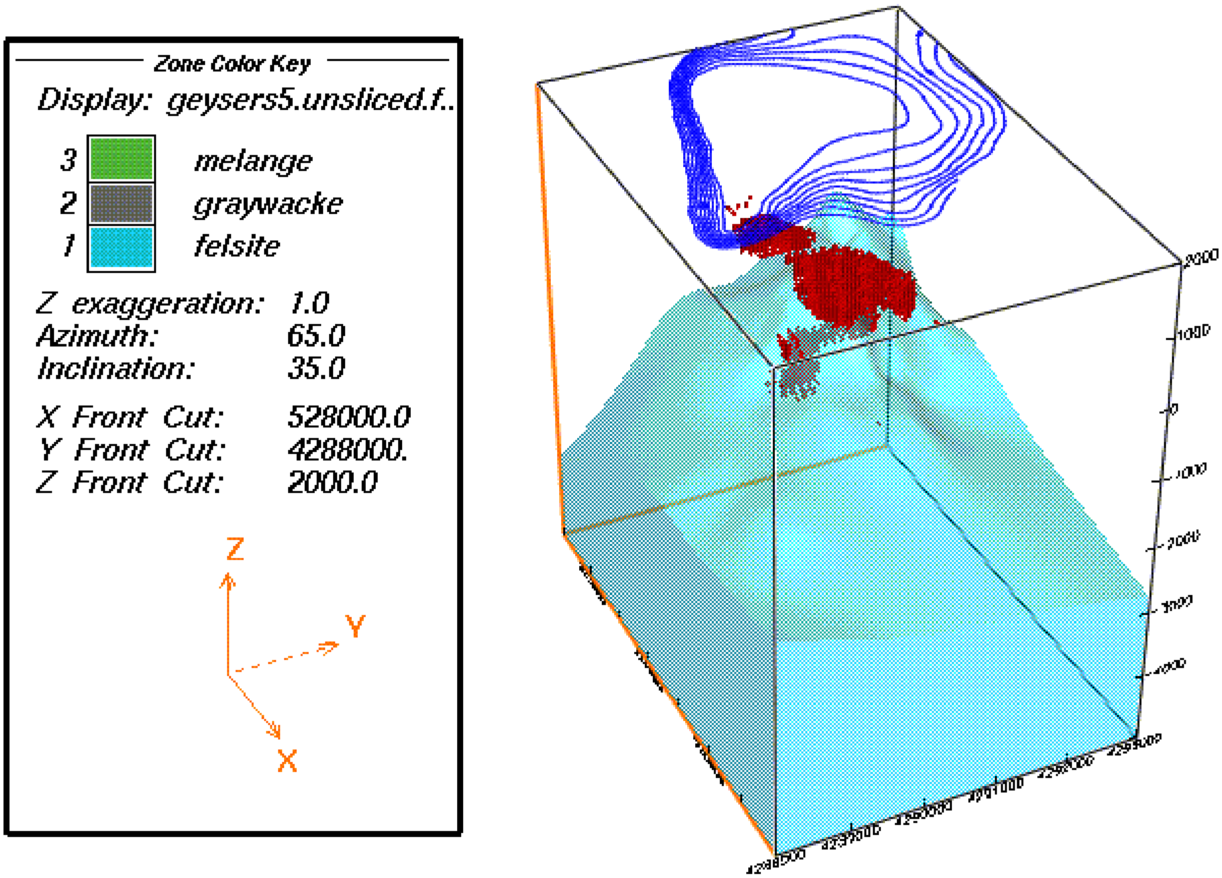
Zone Color Key
Display: geysers5.unsliced.f..
3 melange
2 graywacke
1 felsite
Z exaggeration: 1.0
Azimuth: 65.0
Inclination: 35.0
X Front Cut: 528000.0
Y Front Cut: 4288000.
Z Front Cut: 2000.0
Z
Y
X
2000
1000
0

Figure 6

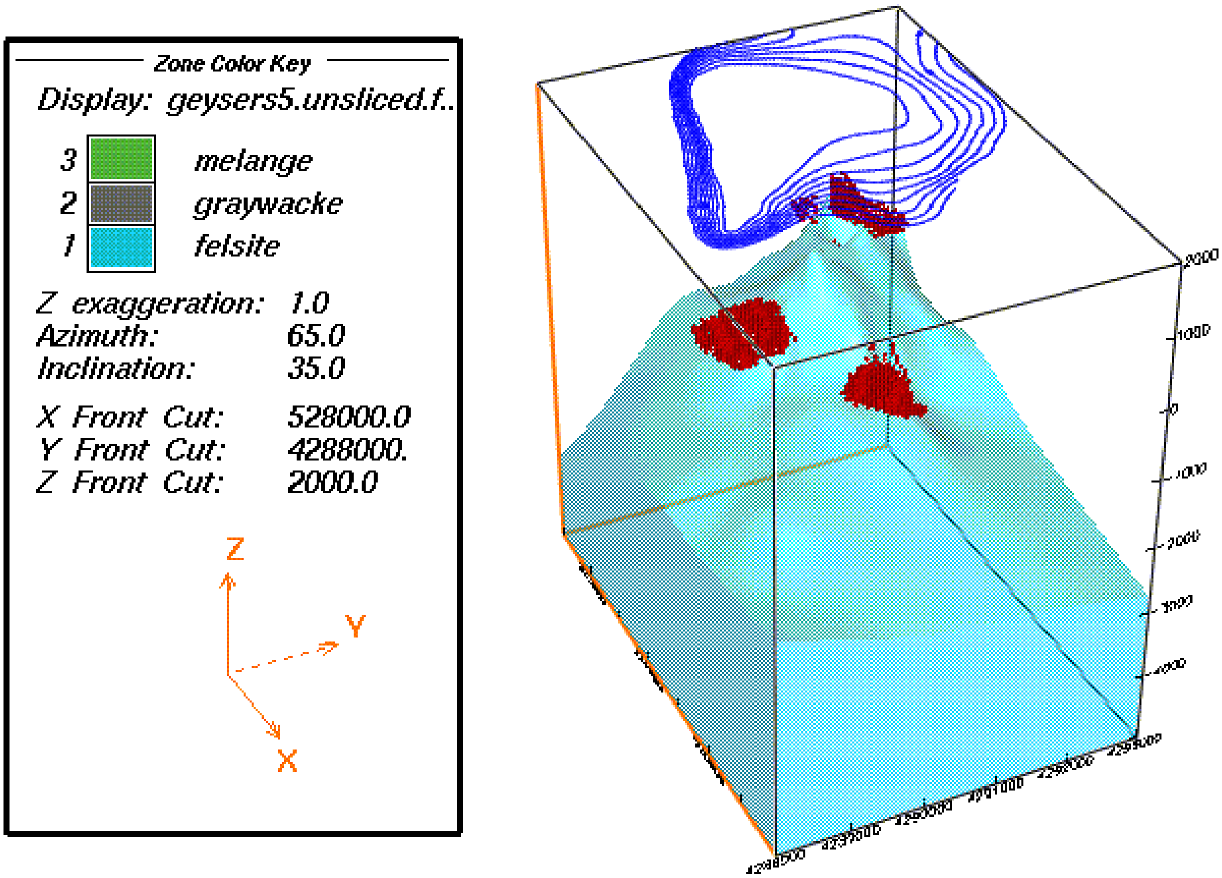
Zone Color Key
Display: geysers5.unsliced.f..
3 melange
2 graywacke
1 felsite
Z exaggeration: 1.0
Azimuth: 65.0
Inclination: 35.0
X Front Cut: 528000.0
Y Front Cut: 4288000.
Z Front Cut: 2000.0
Z
Y
X

Figure 7

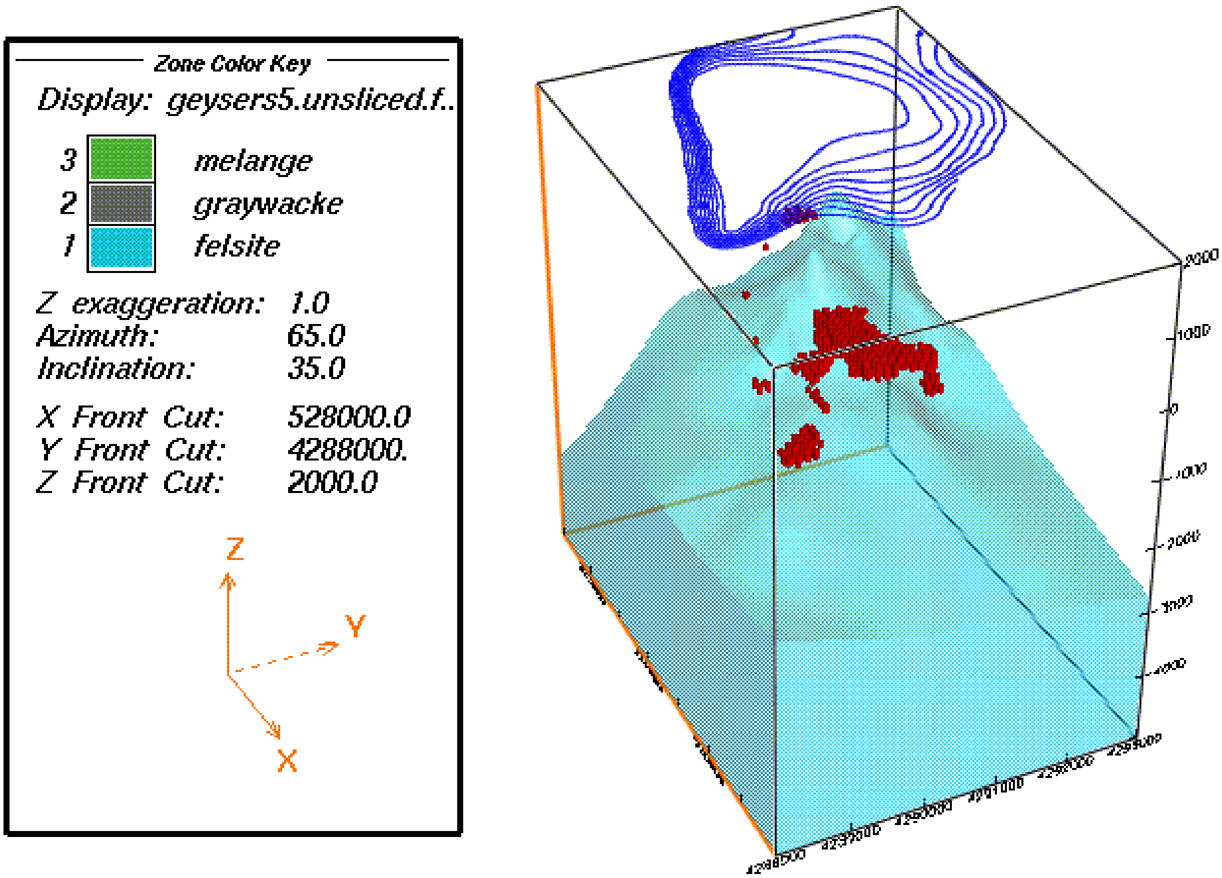

Zone Color Key
Display: geysers5.unsliced.f..
3 melange
2 graywacke
1 felsite
Z exaggeration: 1.0
Azimuth: 65.0
Inclination: 35.0
X Front Cut: 528000.0
Y Front Cut: 4288000.
Z Front Cut: 2000.0
Z
Y
X

Figure 8

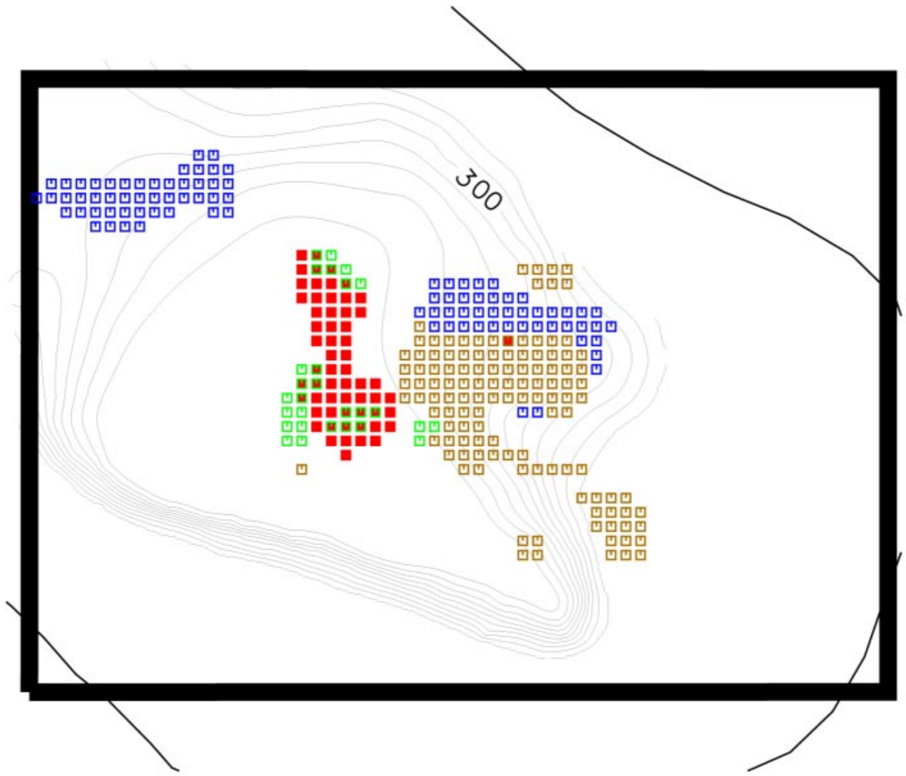

Figure 9